Internal Report No. 66
January 1976

NEUTRON-INDUCED BACKGROUND IN THE ELECTRON/ISOTOPE SPECTROMETER

by

R. A. Mewaldt

Internal Report #66
R. A. Mewaldt

Neutron-Induced Background in the Electron/Isotope Spectrometer

I. Introduction

Analysis of in-flight and laboratory calibration data from the Caltech Electron/Isotope Spectrometer (EIS) on Imp-7 has provided evidence for the importance of a "background" component resulting from the nuclear interaction of energetic neutrons within the detector stack. The low-energy protons and alpha particles produced in these reactions may simulate the characteristics of "real" events due to externally incident charged particles. This internal report presents a preliminary summary of evidence relating to the neutron background component, and points out some of its implications for low-energy cosmic-ray measurements performed with solid-state detector telescopes.

II. In Flight Observations of the EIS Neutron Background

In-flight evidence for neutron-induced events in the EIS (Figure 1) has been obtained from the Neutral Particle Mode, which is triggered by D7. Figure 2 shows raw measured pulse-height distributions over the energy range 0.16 to 100 MeV, obtained from $\sim$ 1 month of quiet time data. The four distributions are for events triggering from 1 to 4 detectors. Since all other detectors including D11 are in anticoincidence, the events must be induced by neutral particles. Taken together, the four distributions suggest that 2 distinct neutral components are responsible for these events. The low energy component dominating below several MeV is known to be due to γ-rays which produce secondary electrons (mainly by the Compton effect) within the detector stack (Hurford et al. 1974). The high energy component, involving energy losses of $\sim$ 2 up to $\sim$ 100 MeV in a single 1 mm detector, is due to energetic charged nuclear products of neutron induced reactions within the detector system. The location of the relative maxima in the distributions and range-energy considerations indicate that the major contribution is from (n,p) reactions.

The Neutral mode counting rates of both the γ-ray and neutron components varied by $\sim \pm$ 10% over a one year period, and both showed excellent correlation with ground based neutron monitors, including periods of Forbush decreases. Thus the time dependence of both components was consistent with secondary production by the interaction of high energy cosmic rays in the material of the spacecraft.

Figure 3 compares the D7 neutral pulse height distribution with distributions measured in two other 1 mm detectors, D0 and D5. These three distributions were obtained during the nine days having the lowest 1.3 - 2.3 MeV proton counting rates observed during the first year of IMP-7 operation (see Mewaldt et al. 1975). Notice that the D5 pulse height spectrum is essentially identical to the D7 spectrum, while the D0 spectrum is somewhat greater, especially at the lowest ($\leqslant$ 2 MeV) and highest ($\geqslant$ 20 MeV) energies. All three detectors have approximately equal active volumes and from laboratory calibrations we expect their γ-ray and neutron responses to be similar. The excess D0 counting rate at $\leqslant$ 2 MeV is due to low energy interplanetary electrons (Hurford et al. 1974), while the excess rate at $E \geqslant 60$ MeV has been shown to be due mainly to an enhanced flux of low energy nitrogen and oxygen nuclei.

Cosmic ray nuclei incident on D0 produce energy losses of $E \leqslant 12.5$ MeV for protons and $E \leqslant 50$ MeV for alpha particles, and might be expected to produce noticeable breaks in the D0 pulse height spectrum at the end of range points. Such a break is visible at the α-particle end of range

(50 MeV), suggesting a finite flux of < 12.5 MeV/nucleon alpha particles at this time. At 12.5 MeV, where the neutron background level is higher, no such break is visible, and comparison with the D5 and D7 spectra suggests that neutron background dominates the D0 pulse height spectrum for $4 \leqslant E \leqslant 20$ MeV. The dashed line in Figure 3 indicates the D0 spectrum obtained during a small energetic solar particle event, when the rate of 4-12.5 MeV protons measured in Narrow Geometry (D2D5) was $\sim$ 50 times its minimum quiet time rate. The D5 and D7 spectra did not increase significantly during this event.

Confirmation of the large background contribution to D0 is possible using independent measurements of the 2.4-12.7 MeV/nucleon cosmic ray ^{1}H and ^{4}He spectra, obtained from the narrow geometry D2D5 coincidence mode of the EIS. Figure 4 shows the expected cosmic ray contributions to D0 for these two quiet-time periods (See Mewaldt <u>et al</u>. 1975a). Also shown in Figure 4 is the D0 spectrum from Figure 3, and a smooth curve representing the average D5 and D7 spectra in Figure 3. Note that the D2D5 observations show that only $\sim$ 10% of the $\sim$ 2 to 12.5 MeV D0 events can be due to cosmic ray protons. Beyond the proton end of range the neutron background is somewhat lower, and it appears that $\sim$ 50% of the $\sim$ 24 to 50 MeV D0 events result from cosmic ray ^{4}He nuclei. The D0 spectrum at 50-100 MeV and beyond also contains significant contributions from cosmic ray nuclei with $Z \geq 3$. We conclude that reliable measurements of low energy ^{1}H and ^{4}He spectra can be made in the D0 single parameter analysis mode <u>only</u> when the fluxes are significantly above their minimum quiet-time levels.

The multi-detector events in Figure 2 imply a corresponding background in the Narrow and Wide Geometry modes. Such events are evident in the 2-dimensional matrices of, for example, D5D6 and D0D1 events, at locations removed from the known H and He isotope response tracks. Further evidence for the neutral particle origin of this background comes from the fact that the count rate of such events in D5D6 and D0D1 is comparable, while the geometry factors differ by a factor of $\sim$20. Although the relatively smooth character of this background does not obscure the proton mass peak in D0D1, the background for less abundant ^{2}H is formidable. Fortunately, the relative background contribution decreases rapidly for longer range events.

III. Neutron Calibrations of the EIS Detector Stack

In order to study the characteristics of neutron-induced background events the spare EIS detector stack was exposed to a 1 Curie Pu-Be neutron source, giving $\sim 1.4 \times 10^{6}$ neutrons/sec. The Pu-Be neutron spectrum (Figure 5) measured by Broek and Anderson (1960), extends to $\sim$ 11 MeV with relative maxima at $\sim$ 3, 4.5, 7.5 and 10 MeV. The source also produces γ-rays up to 4.6 MeV. Figure 6 shows the energy loss spectrum measured in D7 with all other detectors including D11 in anticoincidence, when the source was in back of the detector stack at an angle of 150° to the telescope opening. Essentially identical spectra were obtained in all other 1 mm detectors in the stack including D0 and D5. No significant spectral or count rate differences were observed when the source was placed at other angles relative to the detector stack. Runs with a ^{252}Cf fission neutron source produced similar results. However, the much softer ^{252}Cf neutron spectrum is not as favorable for studying these events.

Neutron induced events were also observed in D2, as shown in Figure 7. The 3-8 MeV D2 count rate is ~ 2% of the corresponding rate in D7. Such events would be interpreted as alpha particles in this single parameter analysis mode.

Neutron induced reactions in silicon detectors of somewhat different design have been studied extensively in the past (see for example Rydin, 1968). In silicon of normal isotopic composition, the most important reactions for producing energetic charged particles are ^{28}Si (n,p) ^{28}Aℓ (Q = 3.85 MeV), ^{28}Si (n,α) ^{25}Mg (Q = 2.65 MeV), and ^{29}Si (n,α) ^{26}Mg (Q = .045 MeV). Silicon-nuclei recoil due to elastic neutron scattering may also be important.

A calculation of the expected energy spectrum of charged products in D7 was performed using the Pu-Be neutron spectrum of Broek and Anderson and the measured D7 active volume of 0.32 cm^3. Neutron cross sections, obtained from the National Neutron Cross Section Center were based primarily on the work of Grimes (1969), Mainsbridge et al. (1963), and Andersson-Lindström (1964). Reactions leading to excited states of the product nucleus were explicitly included.

The result of the calculation is also shown in Figure 6. Above ~ 2 MeV the agreement in the shape of the spectrum and in the absolute counting rate is excellent considering the unsophisticated experimental setup and uncertainties in the neutron cross sections. The sharp rise in the measured spectrum below ~ 1.5 MeV is due mainly to Compton recoil electrons resulting from γ-rays produced by the Pu-Be source. This contribution was not included in the calculation.

A second experiment was performed to observe the beta activity of $A\ell^{28}$ nuclei (mean life = 200 sec) produced by ^{28}Si (n,p) $^{28}A\ell$ reactions within the detectors. The majority of $A\ell^{28}$ β-decay electrons (maximum energy 1.9 MeV) will be above the 0.16 MeV detector thresholds. In this experiment the stack was exposed to the neutron source at a distance of 10 cm for $\sim$ 20 minutes, after which the source was quickly removed from the room. Figure 8 shows the time dependence of the counting rate obtained from the OR'ed outputs of the six detectors D4 through D9. A quiescent background level of 0.58 counts per second has been subtracted. The exponential decay provides conclusive evidence for the ^{28}Si (n,p) $^{28}A\ell$ reaction. The absolute count rate (t = 0) was within 10% of that predicted from cross section data and the Pu-Be source strength.

In addition to the single detector events considered above, exposure of the EIS to the Pu-Be source also produced a small number of events triggering both D2 and D5, where multi-parameter particle identification is possible. An apparent mass can be calculated for each of these events. Although this calibration data is still under study, some preliminary conclusions can be drawn. The count rate of proton-like events (mass = 0.8-1.2 amu), depends critically on the angle of the source with respect to the stack. The count rate is at a maximum at $\theta = 0^0$, suggesting reactions in inactive material in front of D2; for example, knock-on protons from the Mylar window. At backward angles, more characteristic of the neutrons expected from the spacecraft, only a small fraction of the events lie on the proton track. Few α-like events were observed, as expected from range-energy considerations.

Although the relatively crude nature of these calibrations does not permit a detailed evaluation of the neutron response of the EIS instrument, some important conclusions can be drawn:

1) Neutron-induced nuclear reactions within cosmic ray telescopes composed of silicon solid state detectors produce energetic charged products whose subsequent energy-loss characteristics may be identical to those of energetic cosmic rays entering the front of the telescope.

2) At the neutron energies considered (0-11 MeV), the dominant reactions for producing background in the 1 mm detectors of the EIS take place in the active volume of silicon itself, and not in inactive material surrounding the silicon detectors. This conclusion follows from:

   a) The good agreement between the calculations of n-Si reactions and the measurements of 1) the energy loss spectrum and 2) the absolute count rate.

   b) The observation of $A\ell^{28}$ β-decay activity following exposure of the stack to neutrons.

   c) All 1 mm detectors showed generally consistent count rates, independent of the angular orientation of the neutron source.

3) For the neutron spectra considered, the event rate in the 50μ detector D2 is significantly greater than expected from neutron reactions in its active volume alone, suggesting that contributions from surrounding inactive material may dominate when the range of the charged reaction products is significantly greater

than the detector thickness. Note that the ratio of the D2 to D7 active volumes is 0.01 the active-area ratio is 0.2, while the observed 3-8 MeV count rate ratio was ~ 0.02. We therefore conclude that it is not possible to simply scale the neutron-induced energy-loss spectrum between silicon detectors of different size without detailed knowledge of their environment, and the incident neutron spectrum.

4) Neutron induced nuclear interactions also produce multi-detector events. However, for D25 events in the EIS, only a small fraction of these events is likely to be confused with real proton events. Such events may, however, produce an important background in the ^{2}H and ^{3}H mass regions.

IV. Discussion

The calibrations and in flight measurements with the EIS suggest that a neutron produced background will be present to some extent in all low energy cosmic ray experiments. Although this background contribution will in general depend on the size, composition, and geometry of the active detectors, as well as on the composition and geometry of passive material in and around the experiment, first order estimates of the neutron background in other detector systems are possible.

The count rate R(E) (MeV^{-1} sec^{-1}) of events with energy E due to neutron interactions in a single detector of area A, thickness t and volume V=At can be represented as R(E) = VF(E), where F(E) is an integral over the incident neutron spectrum and reaction cross sections. The equivalent flux $J_b(E)$ due to this background contribution is $J_b(E) \simeq R(E)/A\Omega \simeq (\frac{V}{A\Omega})F(E)$, where $A\Omega$ is the detector's geometry factor ($cm^2 sr$) for incident cosmic ray nuclei. Thus the relative neutron background contribution in a detector will scale roughly as its volume to geometry-factor ratio. For spacecraft of mass and design similar to IMP-7, we can estimate F(E) for silicon detectors from the D7 spectrum in Figure 2 using $F(E) = R(E)/V$ and the D7 volume of 0.33 cm^3. Such estimates imply that unless the volume to geometry-factor ratio is at least an order of magnitude smaller than the EIS D0 ratio of ~ 0.17 cm/sr, single detector measurements of the quiet time proton flux at ≈5 MeV will likely be dominated by background.

A similar procedure can be followed for scaling the γ-ray background in Figure 2 to other detector systems. At energies where Compton scattering dominates, extension to detectors of other composition is straight forward.

The above procedure neglects background contribution from interactions in passive material within the detector system. Such contributions will be instrument dependent, but appear to be of secondary importance in the 1 mm detectors of the EIS. Although we might also expect some dependence of the neutral background rate on the total mass and location of material within the spacecraft, the IMP-7 mass (~ 400 kg) is typical of many recent spacecraft.

By appropriately combining events that trigger D7 and D6, D8, and D9 it is possible to approximate the response of larger volume silicon detectors up to 4 mm thick. Figure 9 shows the relative neutral event rate per unit volume in 3 energy ranges for detectors from 1 to 4 mm thick. It appears that the event rate scales with detector volume reasonably accurately as long as the proton range is not significantly greater than the detector thickness

Note that the neutron background is relatively constant in time. Extrapolation of the observed dependence on the Mt. Washington neutron monitor suggests that the background component will vary by approximately a factor of 2 over the solar cycle, a variation comparable to that of the integral cosmic ray flux. (See Webber, 1967).

Single parameter measurements are especially susceptible to this background. For example, if all D0 events in Figure 3 with energy loss of $\sim 4 - 50$ MeV are interpreted in terms of the calibrated proton and alpha response of the instrument ($A\Omega = 1.8\ cm^2 sr$), the resulting 4 - 12.5 MeV/nucleon fluxes are ~ 10 times higher than those based on the EIS Narrow Geometry (D2D5) analysis for this period (see Mewaldt et al. 1975). The resulting spectra have negative slopes with $\gamma \simeq -2$ to -3. Thus, neutron-induced background may have relevance for some reported quiet-time measurements in the "low-energy turnup" region.

Laboratory calibrations of the EIS with low energy neutrons (Section III) imply that D2 will also have an in-flight neutron-induced background level. However, since the ratio of D2 to D7 active volumes is $\sim 1\%$, while the active area ratio is $\sim 20\%$, it is not possible to simply scale the observed D7 neutron background to D2 without accurate knowledge of the relative contribution of various possible sites of the neutron interactions responsible for events produced in the individual detectors. A related complication is that the maximum energy loss of any charged particle in D2 is only about 1/6 the maximum energy loss in D7. Calculations of the relative response are therefore very difficult without some knowledge of the spacecraft produced neutron spectrum. Ignoring these considerations for the moment, note that calibrations with the Pu-Be neutron source gave a ratio of D2/D7 ~ 0.02 for events with pulse height of 3-8 MeV. Taking 2% of the inflight D7 3-8 MeV event rate gives a predicted D2 event rate of $\sim 4 \times 10^{-6}$ sec^{-1}, compared to the minimum observed event rate of $\sim 10^{-5}$ sec^{-1}. It thus appears that a significant fraction of our minimum observed count rate of D2 α-like events may be neutron background.

Multi-parameter particle identification can be very valuable in supressing the importance of neutron induced events. Because the angular distribution of nuclear reaction secondaries extends over 4π, only a fraction of the background events satisfying multi-detector coincidence requirements will fall on the mass tracks of stable isotopes. This background may be significant, however, for relatively rare isotopes such as ^2H and ^3H. It is also conceivable that concentrations of passive material within the angular acceptance cone of a detector system could produce spurious peaks in the mass spectra.

V. Acknowledgements

C. Chang, W. R. Cook, E. Gustafson, G. J. Hurford, R. Sullivan and S. B. Vidor made important contributions to various aspects of this work.

VI. References

Anderson-Lindstrom, G., Thesis, University of Hamburg (1964), see also BNL-325.

Broek, H. W., and C. E. Anderson, Rev. Sci. Inst., 31, 1063, 1960.

Grimes, S. M., Nuc. Phys. A124, 369, 1969.

Hurford, G. J., R. A. Mewaldt, E. C. Stone, and R. E. Vogt, Ap.J., 192, 541, 1974.

Mainsbridge, B., T. W. Bonner, and T. A. Rabson, Nuc. Phys. 48, 83, 1963.

Mewaldt, R. A., E. C. Stone, and R. E. Vogt, Proc. 14th Int'l. Cosmic Ray Conf. Munich, 2 , 774, 1975.

Rydin, R. A., in Semiconductor Detectors, ed. by G. Bertolini and A. Coche, Wiley Interscience, New York, 409, 1968.

Stewart, L., Phys. Rev. 98, 740, 1955.

Webber, W. R., Handbuch der Physik, XLVI/2, 181, 1967.

FIGURE CAPTIONS

FIGURE 1 Cross-section of the IMP-7 EIS. Detectors D0 through D10 are 1 mm thick silicon surface-barrier detectors, except for D2, which is 50 μ thick. D11 is a plastic scintillator.

FIGURE 2 Pulse-height distributions for Neutral Mode events obtained from ~ 1 month of quiet-time flight data during early 1973. Neutral mode events must satisfy the logic requirements {D0D1D3D4D5} D7 {D10D11} where the angular brackets mean "not fired". In this mode the sum of the energy losses in D6 through D9 is obtained. Note the use of scale factors for some of the spectra.

FIGURE 3 Uncorrected pulse-height distributions for D0, D5, and D7 obtained during February 7-10, 1973 and March 7-11, 1973. All other detectors are in anticoincidence. The dashed line shows the D0 spectrum obtained during a small solar proton event.

FIGURE 4 Contribution of 2.4-12.5 MeV/nucleon ^{1}H and ^{4}He cosmic ray nuclei to the quiet time D0 counting rate. The dashed line represents an average of the D5 and D7 points in Figure 3.

FIGURE 5 Neutron spectra from a Pu-Be source. Top Panel: Stewart (1955). Botton panel (dashed): Broek and Anderson (1960).

FIGURE 6 Measured and calculated pulse-height spectra in D7 due to neutrons from the Pu-Be source. Source distance = 29 cm.

FIGURE 7 Measured pulse-height spectrum in D2 due to Pu-Be neutrons.

FIGURE 8 Time dependence of the (D4+D5+D6+D7+D8+D9) counting rate after exposure to the Pu-Be source at a distance of ~ 10 cm. The source was removed at time t = 0.

FIGURE 9 Relative count rate per unit volume for detector thickness > 1 mm as estimated from neutral events triggering D6-D9.

IMP-7
CALTECH ELECTRON/ISOTOPE SPECTROMETER

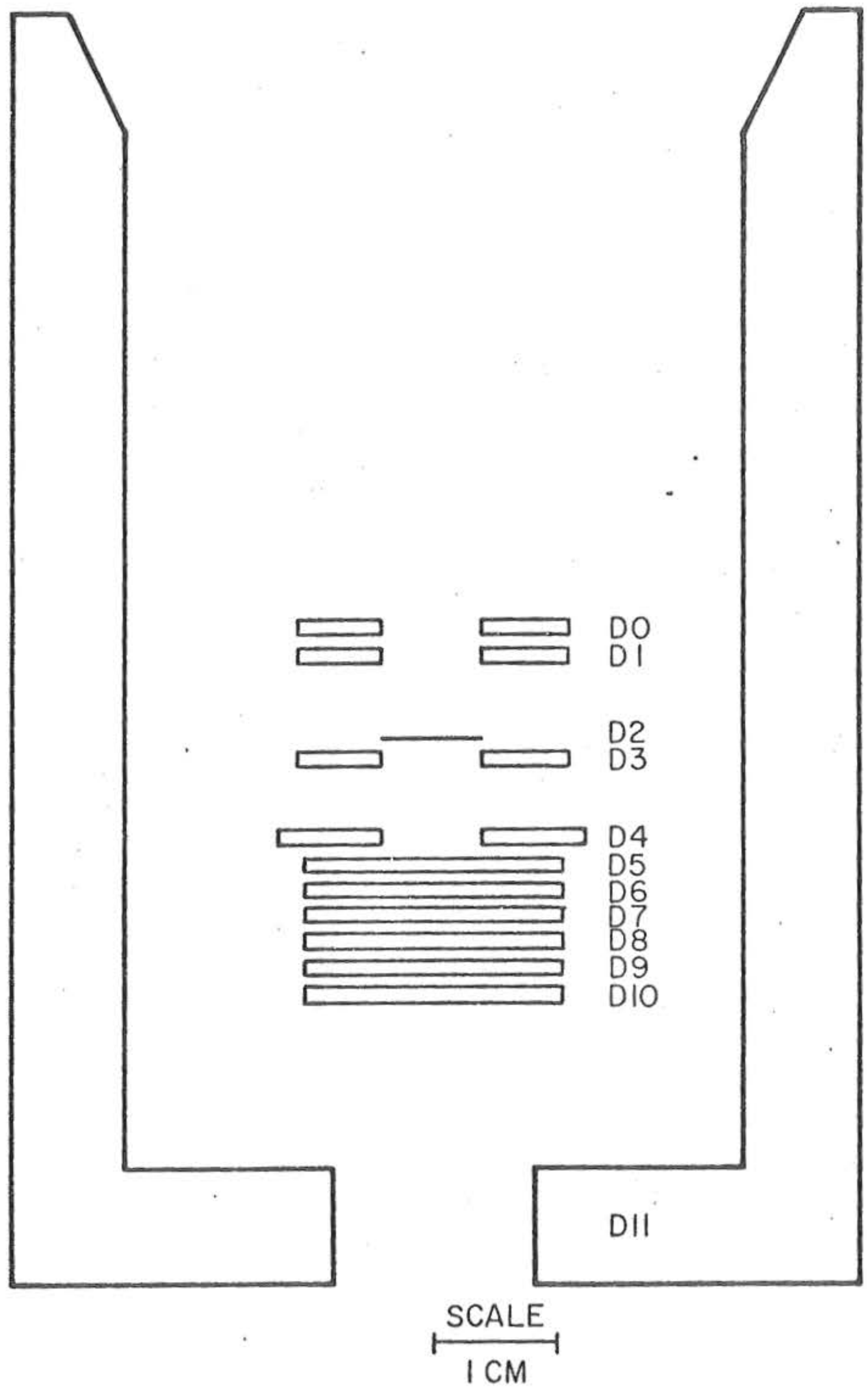

FIGURE 1

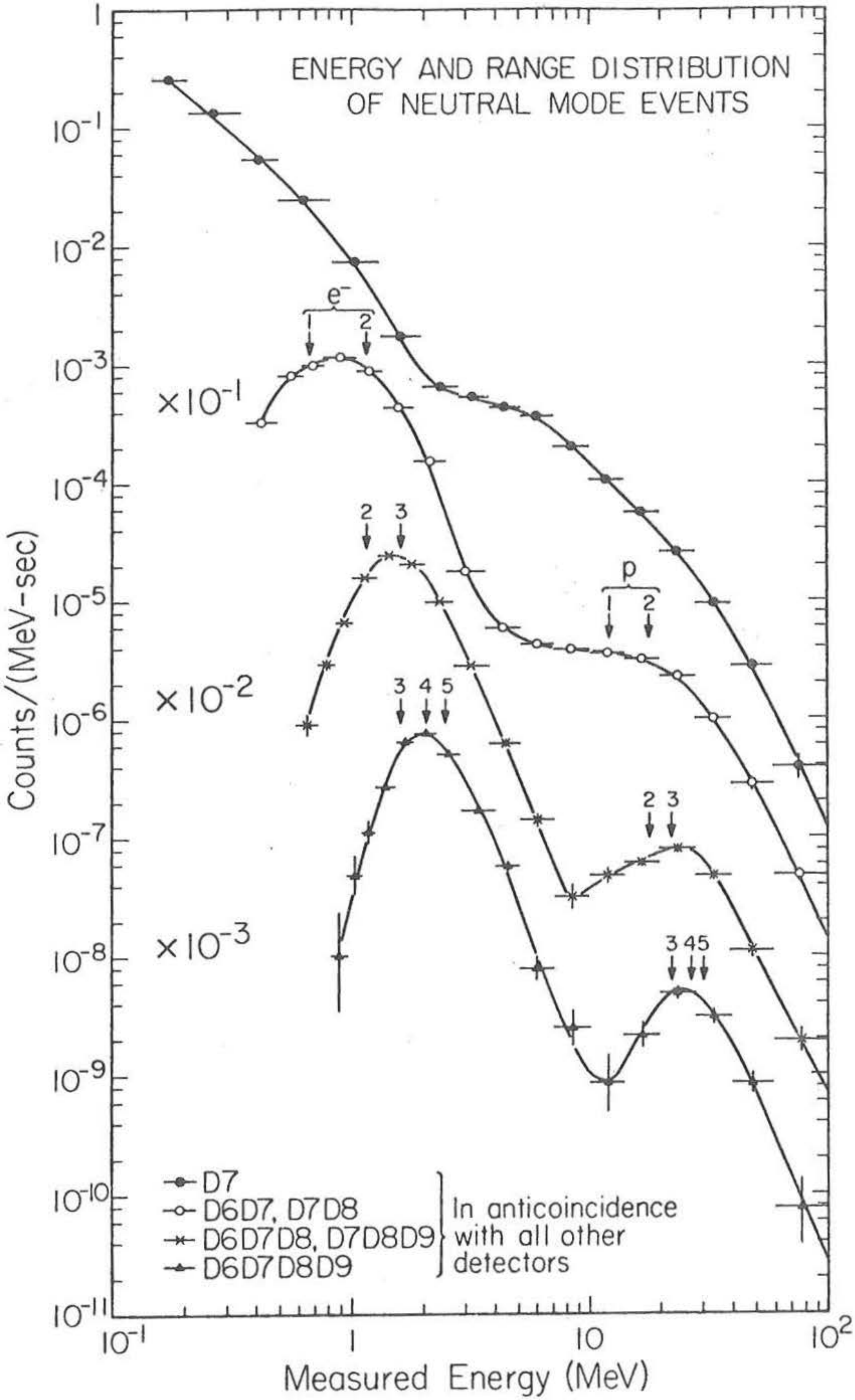

ENERGY AND RANGE DISTRIBUTION
OF NEUTRAL MODE EVENTS
Counts/(MeV-sec)
Measured Energy (MeV)
×10⁻¹
×10⁻²
×10⁻³
e⁻
p
D7
D6D7, D7D8
D6D7D8, D7D8D9
D6D7D8D9
In anticoincidence with all other detectors

FIGURE 2

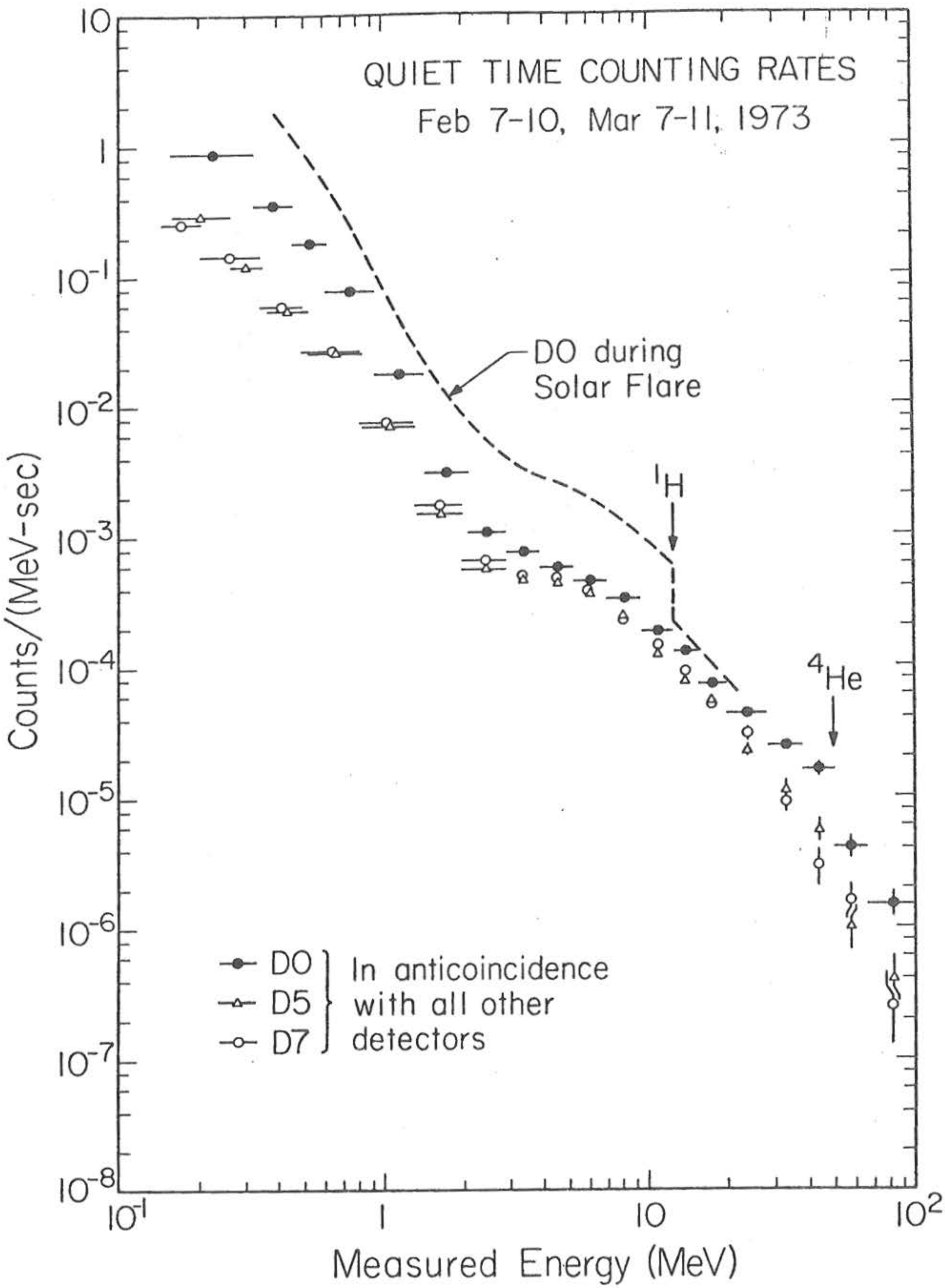
QUIET TIME COUNTING RATES
Feb 7-10, Mar 7-11, 1973
DO during
Solar Flare
^1H
^4He
D0
D5
D7
In anticoincidence
with all other
detectors
Counts/(MeV-sec)
Measured Energy (MeV)
10
1
10^{-1}
10^{-2}
10^{-3}
10^{-4}
10^{-5}
10^{-6}
10^{-7}
10^{-8}
10^{-1}
1
10
10^2

FIGURE 3

FIGURE 5

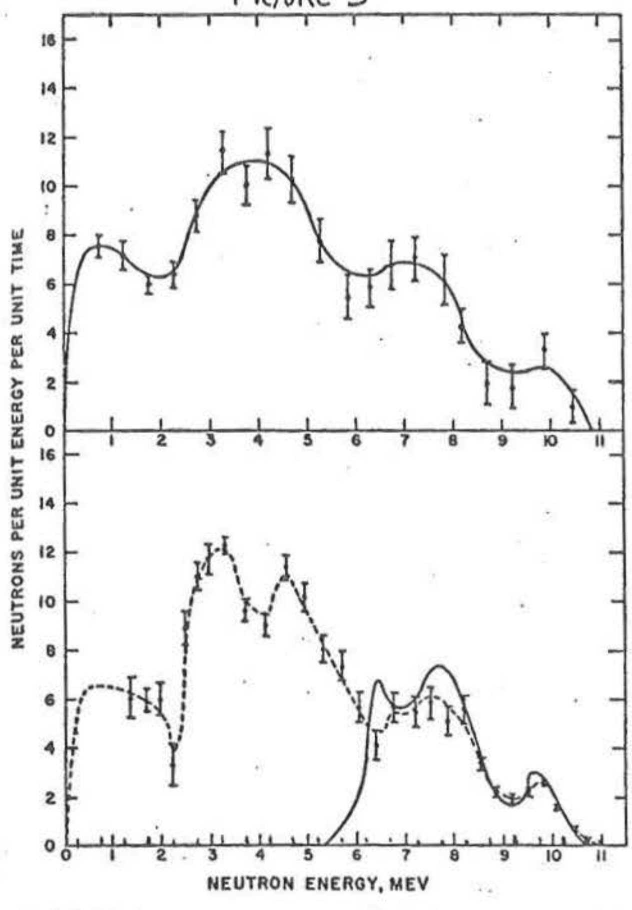

[redacted] Neutron energy spectrum of a Pu-Be source. The upper graph is Stewart's data (reference 22). The lower graph is the measurement described in the text (dotted), and the calculated part of the spectrum due to Be^{9} (α,n) reaction leaving C^{12} in its ground state (solid). (RSI 21, 1063, A6D)

FIGURE 5

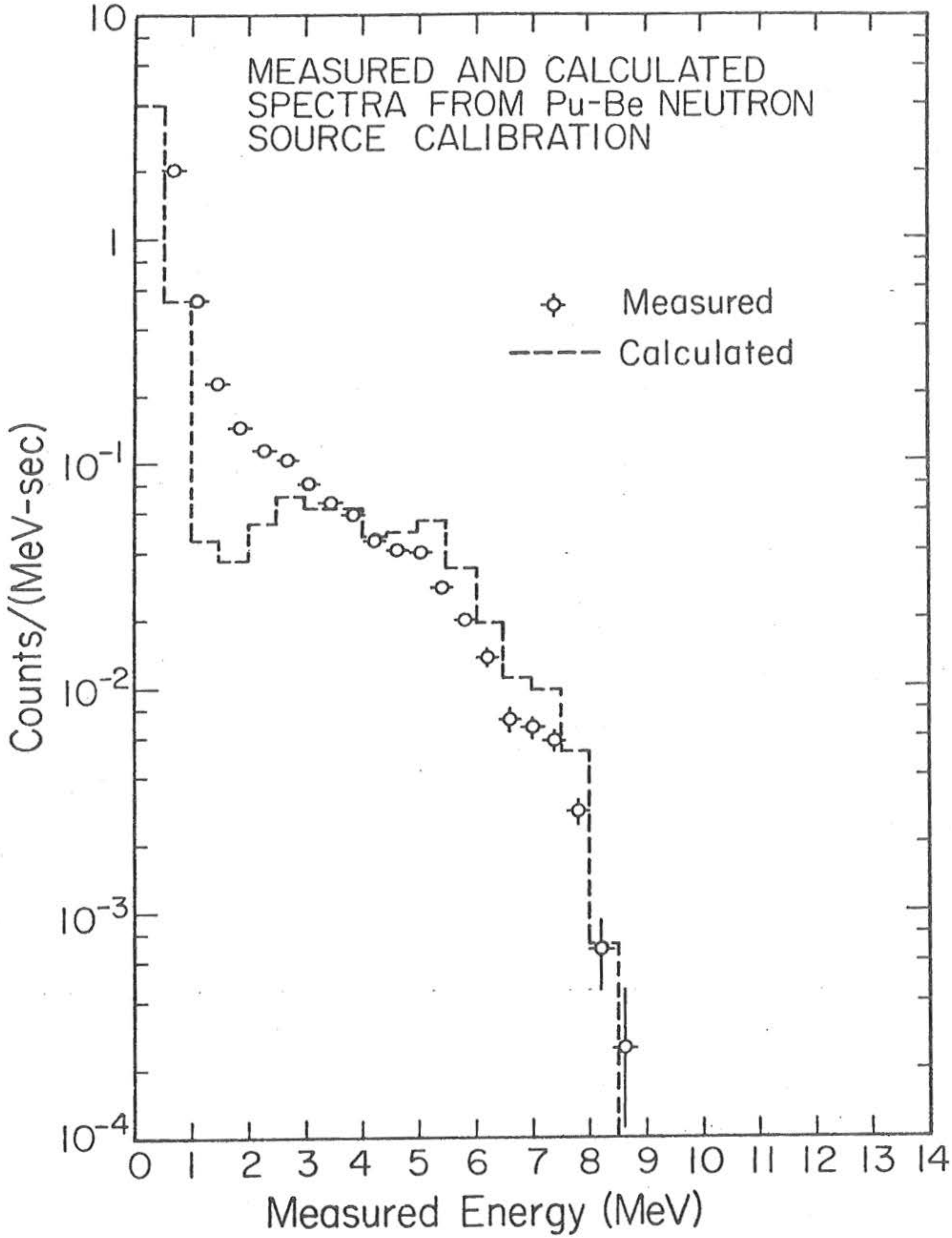
MEASURED AND CALCULATED
SPECTRA FROM Pu-Be NEUTRON
SOURCE CALIBRATION
Measured
Calculated
Counts/(MeV-sec)
10
1
10^-1
10^-2
10^-3
10^-4
0 1 2 3 4 5 6 7 8 9 10 11 12 13 14
Measured Energy (MeV)

FIGURE 6

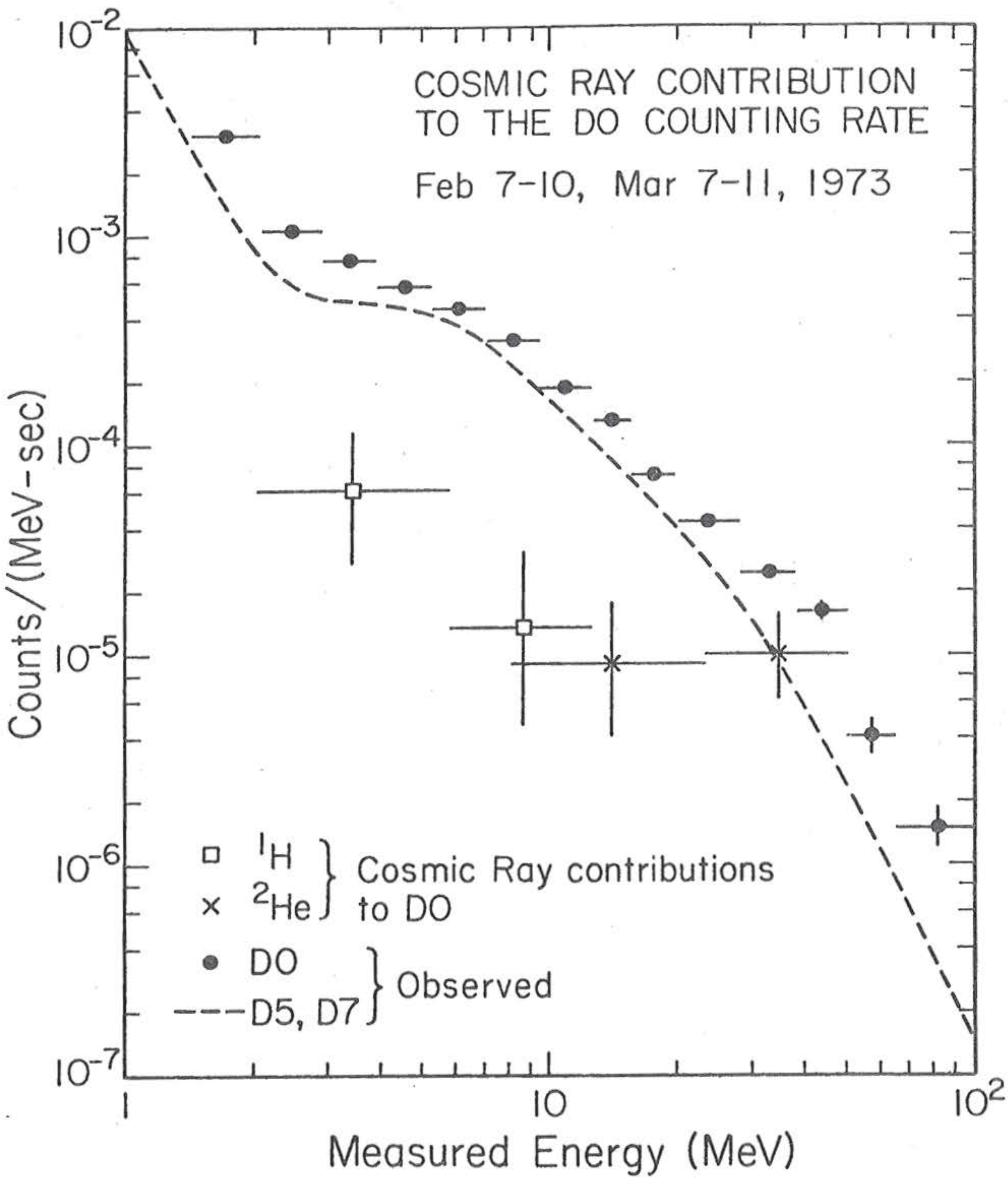
COSMIC RAY CONTRIBUTION
TO THE DO COUNTING RATE
Feb 7-10, Mar 7-11, 1973
10^{-2}
10^{-3}
10^{-4}
10^{-5}
10^{-6}
10^{-7}
Counts/(MeV-sec)
1
10
10^2
Measured Energy (MeV)
^1H
^2He
Cosmic Ray contributions to DO
DO
D5, D7
Observed

FIGURE 4

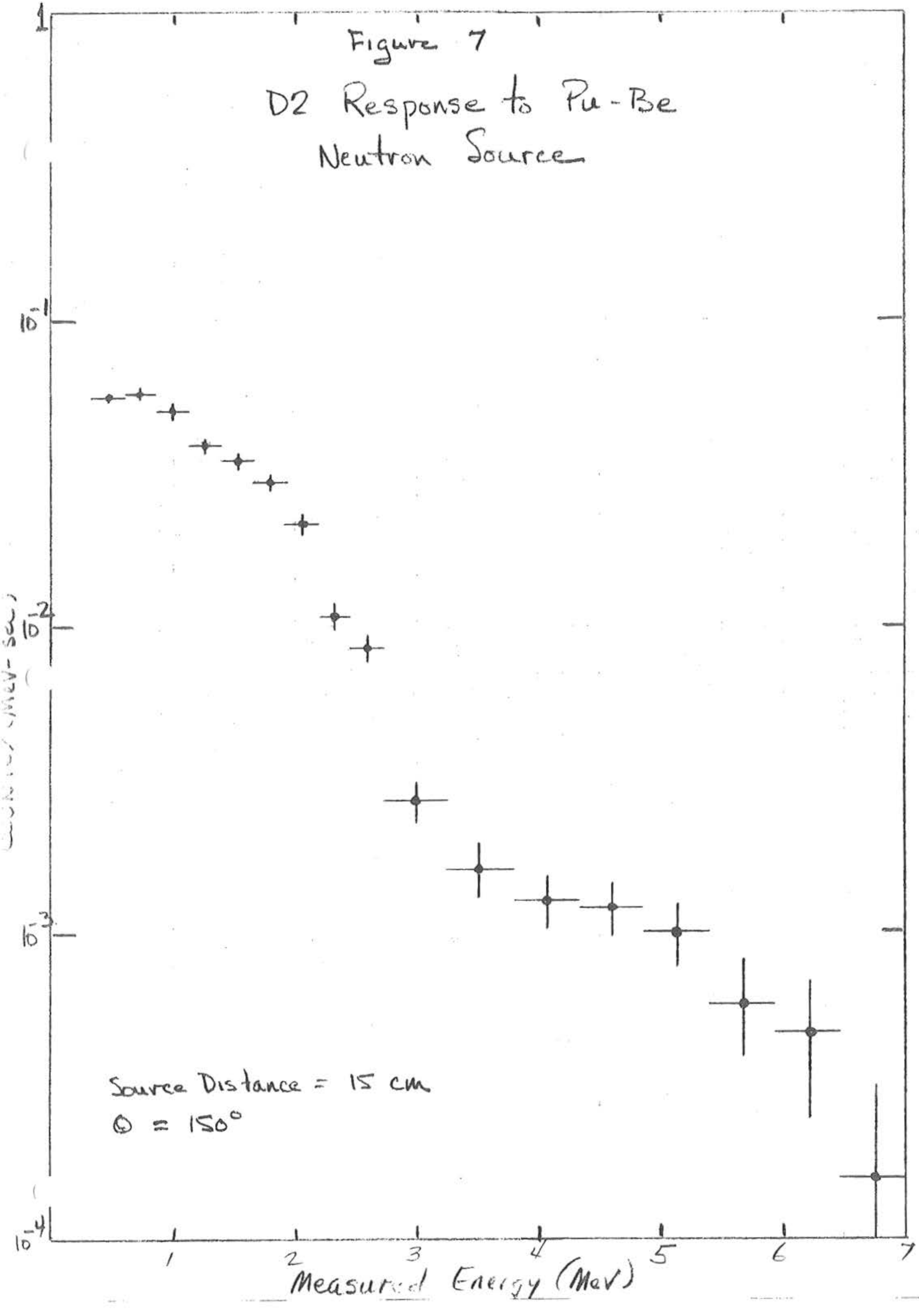

Figure 7

D2 Response to Pu-Be Neutron Source

FIGURE 8

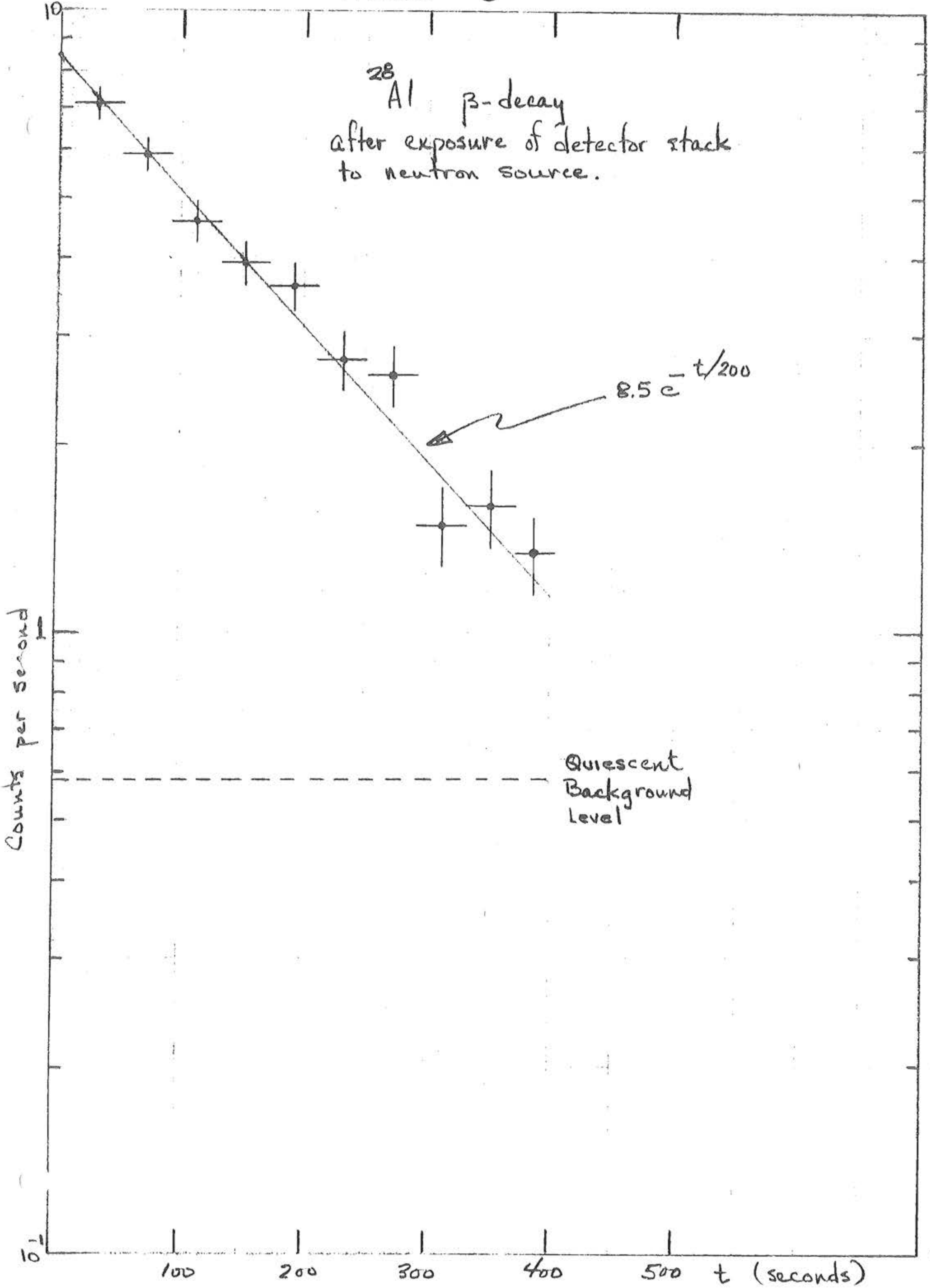

28 Al β-decay
after exposure of detector stack
to neutron source.
8.5 e^{-t/200}
Quiescent
Background
Level
Counts per second
10
1
10^{-1}
100
200
300
400
500
t (seconds)

FIGURE 9

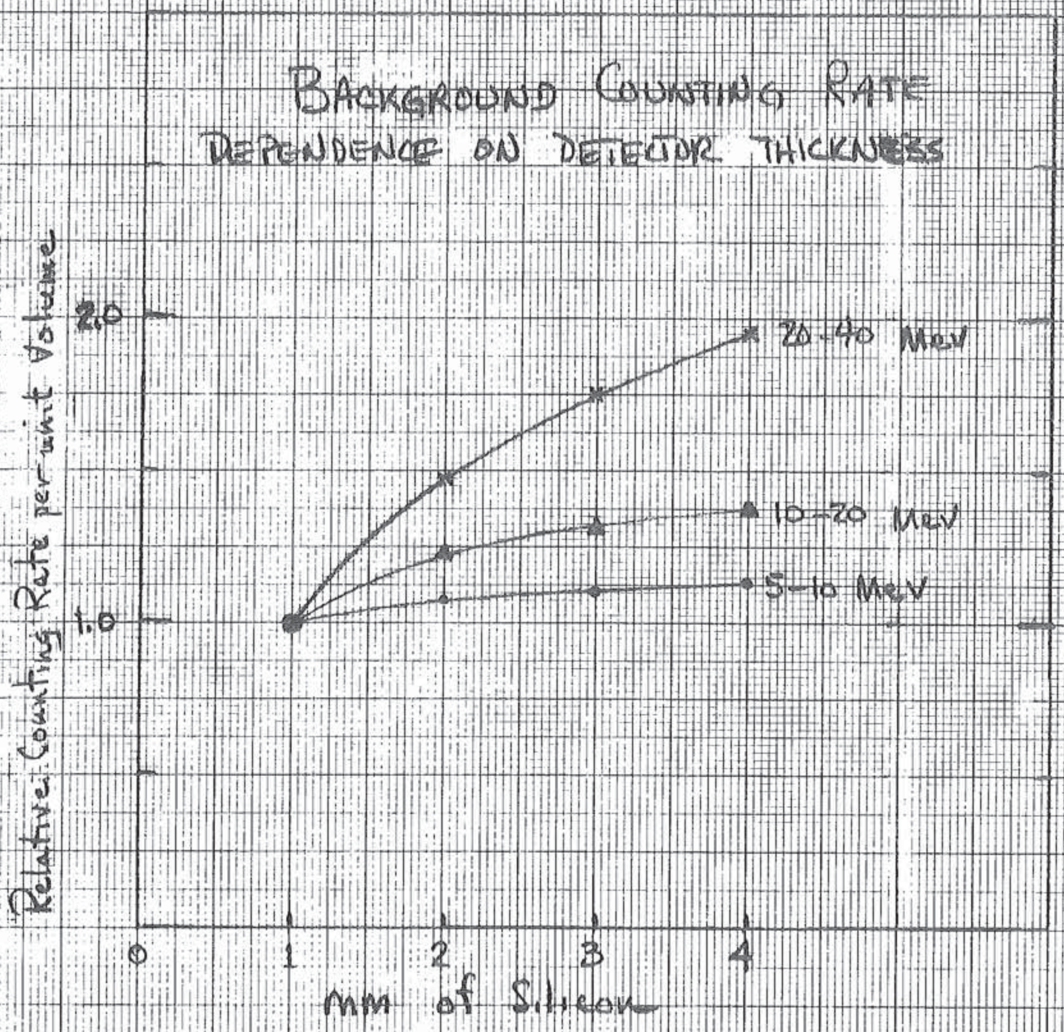

BACKGROUND COUNTING RATE
DEPENDENCE ON DETECTOR THICKNESS
Relative Counting Rate per unit Volume
2.0
1.0
20-40 MeV
10-20 MeV
5-10 MeV
0
1
2
3
4
mm of Silicon